ISSN Print: 2394-7500
ISSN Online: 2394-5869
Impact Factor: 5.2
IJAR 2017; 3(8): 872-876
www.allresearchjournal.com
Received: 12-06-2017
Accepted: 18-07-2017

Mandeep
Department of Chemistry, University of Delhi, Delhi, India

Corresponding Author:
Mandeep
Department of Chemistry, University of Delhi, Delhi, India

Synthesis and characterization of Na/Li containing vanadium oxides

Mandeep

Abstract
Our attempt to synthesize $Na_2V_3O_7$ and $LiVO_3$ by using template free modified solvothermal methods with ethylene glycol-water solvent system (EG:H_2O; 2:1 *v/v*) followed by calcination at 500 °C in air have resulted in the formation of NaV_6O_{15} admixed with NaV_3O_8, phase pure NaV_6O_{15} and $Li_{0.6}V_{1.6}O_{3.67}.H_2O$. The compounds are being analyzed using P-XRD and FE-SEM. NaV_6O_{15} crystallizes in the *A*2/*m* space group with a monoclinic crystal structure while $Li_{0.6}V_{1.6}O_{3.67}.H_2O$ crystallizes in the *I*4/*mmm* space group with a tetragonal crystal structure. Refined lattice parameters of NaV_6O_{15} are a = 10.151(5), b = 3.606(2), c = 15.581(1) Å, β = 109.45° and $Li_{0.6}V_{1.6}O_{3.67}.H_2O$ are a = 3.712(1), c = 15.96(1) Å. The phase pure NaV_6O_{15} and NaV_3O_8 admixed NaV_6O_{15} have rod shaped morphology with an average length of 7 μm and diameter of 0.5 μm.

Keywords: Li-ion batteries, vanadium oxides, Na/Li containing vanadium oxide and modified solvothermal methods

1. Introduction
Energy demand and supply has a significant role in the evolution of civilization [1]. Solar, wind, nuclear power, fossil fuels, hydropower, etc. are used to produce energy in the form of electricity. 80% of the total world energy generation is from fossil fuels, which cause air and water pollution, greenhouse effects from CO_2 emissions and other severe environmental impacts [2]. Therefore, the utilization of renewable energy and the development of more advanced devices for its storage is quite essential and desired. These next generation energy storage devices must possess better performance, like higher power density, energy capacity and longer battery life [3].
Out of different kinds of energy storage devices available, Li-ion batteries (LIB) are drawing more attention in recent years due to high specific energy, cell voltage, good capacity retention and negligibly small self-discharge [2]. Since the commercialization of the first LIB in 1991, LIBs have ruled over the entire electronic appliance market till now, with large applications in portable electronics, power tools, and electric vehicles. Moreover, portable electronics require a longer standby time; on the other hand, electric vehicles require longer travel distance, shorter charging time and longer lifetime [4]. The performance of a LIB is crucially dependent on the type of electrode material used. Hence, it is crucial to develop novel electrode materials of LIBs with the higher power density and performance rate, and longer cycle life. Recently, Na-ion batteries (NIBs) have emerged as another important class of energy storage devices because of the low cost and higher abundance of Na resources [5]. Most of the electrode materials used for the LIBs are not fit for the NIBs due to size difference in Li ion and Na ion [6]. Therefore, it is crucial to develop novel high-performance electrode materials for NIBs [7].
As the conventional layered-crystal structural materials, electrode materials of transition metal based oxides are considered as the most promising for advanced energy storage devices due to their high specific capacity, abundant resources and lower costs [8]. Vanadium based oxides attracted immense attention as electrode material for Li/Na ion batteries because of multiple oxidation state switches of vanadium, easy preparation and low cost. Due to many accessible oxidation states, vanadium oxide-based electrodes intercalate more than one Li^+/Na^+ ions per formula unit, so the specific capacity is improved.

Recently, MnO/C Composite are used to accelerate rate and life of Li ion batteries [9]. Co_3O_4 nanofibres are also used as anode material for LIBs [10].

These, vanadium based oxides have been categorized into: vanadate (Li_3VO_4, $Na_{0.33}V_2O_5$, NaV_2O_5, NaV_6O_{15}, $Na_2V_6O_{16}$, $Na_{1.1}V_3O_{7.9}$ and so on) and vanadium oxides (such as VO_2, V_2O_3, V_2O_5 and so on). The synthesis of vanadium-based material has been carried out using different synthetic routes. Bilayered-V_2O_5 nanobelts synthesized by Wang and Su using the solvothermal method with mixed solvent of pyridine-water, which demonstrated a high reversible capacity of 250 $mAhg^{-1}$ [11]. A template free polyol-induced solvothermal method was applied to synthesize hollow V_2O_5 nanosphere [12]. These V_2O_5 nanospheres showed a discharge capacity of 150 $mAhg^{-1}$ attributed to the insertion of one Na-ion per V_2O_5 formula unit. Mesoporous flake-like β-$Na_{0.33}V_2O_5$ has been successfully prepared by S. Liang [13] and co-workers using a facile hydrothermal reaction at 205 °C with subsequent calcinations which demonstrates high specific discharge capacity of 339 $mAhg^{-1}$ when used as cathode material in Li-ion batteries. NaV_6O_{15} nanoflakes [14] are synthesized by Hanna He *at el*. using facile two-step method, in which $(NH_4)_{0.5}V_2O_5$ nanoflakes are first prepared by hydrothermal approach and then transformed to NaV_6O_{15} by a solid state method. S. Yuan *et al.* prepared Layered $Na_2V_6O_{16}$ nanobelts [15] by facile and template free hydrothermal method using the vanadium oxide and sodium hydroxide as starting materials. When tested as cathode material in sodium ion battery it shows a high reversible capacity of 194.6 $mAhg^{-1}$. $Na_{1.1}V_3O_{7.9}$ nanobelts [16] were synthesized by mixing equimolar quantities of V_2O_5 and NaOH in water and resulted suspension was treated hydrothermally then as synthesized product was calcined. G. Yang *et al.* prepared the orthorhombic Li_3VO_4 with different morphologies using the solvothermal method using the Ethanol-water solvent and stoichiometric amounts of NH_4VO_3 and $LiOH{\cdot}H_2O$ as starting materials. Li_3VO_4 showed potential as an insertion anode material for LIBs with safe and low discharge voltage of 0.75 V vs Li/Li^+ (in average) with a huge capacity of 323 mAh g^{-1} [17].

Synthesizing porous electrodes could also be an effective way for improving the rate performance of a Li/Na-ion battery. Porous materials can be synthesized by two different routes, either using template method which involves surfactants as structure-directing agents (SDAs). The microstructure of the material depends on the choice of the surfactant used. The most common SDAs used are cationic alkyltrimethylammonium type [18], anionic sulfonates [19], mesoporous silica materials KIT-6 [20] and SBA-15 [21] etc. The porosity can also be attained in a template free synthesis which includes methods like electrodeposition [22], ultrasonication [23], hydro or solvothermal synthesis [24, 25]. Porous monodisperse V_2O_5 used as cathode shows greatly improved electrochemical performance [26]. Therefore, we believe that if the strategy of making porous material is extended to other electrodes the battery performance can be improved. So the above literature survey encouraged us to work on the synthesis of novel mesoporous vanadium based oxides using the template free hydrothermal method followed by calcination.

2. Experimental section

2.1 Synthesis of $Na_2V_3O_7$: The synthesis of $Na_2V_3O_7$ was carried out using two different methodologies by solvothermal method. The solvent ethylene glycol-water (EG-H_2O; EG, extrapure-AR purchased from SRL and Millipore water was used) was prepared by mixing EG: H_2O in 2:1 (*v/v*) ratio. 0.9094g of V_2O_5 (Sigma-Aldrich, purity ≥ 99.6%) was added in the EG-H_2O solvent with constant magnetic stirring at room temperature for 30 min. In the first methodology, 1.266g of oxalic acid (Himedia-AR, purity ≥99.5%) was dissolved in 10 mL of solvent in a separate beaker and then added to the V_2O_5 solution under continuous stirring. The yellow color of the solution turned to green on stirring. In the second methodology, 0.25 mL of hydrazine hydrate (Sigma-Aldrich, purity ≥ 80 %) was added dropwise under continuous stirring to the V_2O_5 solution and after the addition of hydrazine hydrate, the yellow color of the solution changed to dull blue.

In a separate beaker, stoichiometric amount (0.266g) of NaOH (Himedia-AR, purity ≥ 98%) was dissolved in 10ml of solvent and added dropwise to each of the above solutions. The solutions were then stirred continuously for 30 min. Then, the resulting solution was transferred to a 50 mL Teflon lined autoclave and kept for solvothermal treatments at 180 °C for 24 hrs. The obtained products were filtered out and thoroughly washed with ethanol after the solvothermal reactions. After washing with ethanol, the products were dried and then calcined in air at 500°C for 12 hrs. The products obtained before and after calcinations were subjected to various analyses.

2.2 Synthesis of $LiVO_3$: $LiVO_3$ was prepared using the solvothermal method in the mixture of ethylene glycol (EG)-water (H_2O); (EG, extrapure-AR purchased from SRL and Millipore water are used) solvent system (prepared by mixing EG: H_2O in 2:1 (*v/v*) ratio). Stoichiometric amounts of V_2O_5 (Sigma-Aldrich, purity ≥ 99%) and $LiOH.H_2O$ (SRL, purity ≥ 99 %) were transferred in separate beakers containing the EG-H_2O solvent system. The V_2O_5 suspension in EG: H_2O was continuously stirred on a magnetic stirrer at 55°C. At the same time, the suspension of $LiOH.H_2O$ was stirred with a glass rod to obtain a clear solution. Finally, the V_2O_5 suspension was mixed with the $LiOH.H_2O$ solution and stirred for another 30 min. The solution prepared was then transferred into the autoclave (of 50 mL capacity) and treated solvothermally at 180 °C for 24 hrs. The compound obtained was filtered, dried and then subjected to the P-XRD analysis.

3. Results and Discussion

3.1 Powder X-Ray Diffraction (P-XRD)

3.1.1 P-XRD patterns of NaV_6O_{15} admixed with NaV_3O_8

The P-XRD patterns obtained for the $Na_2V_3O_7$ stoichiometric preparation using oxalic acid as a reducing agent is shown in the Figure 3.1. The P-XRD pattern of the as-synthesized compound after solvothermal treatment shows the formation of $HNaV_6O_{16}.4H_2O$ along with NaV_6O_{15}. Analysis of the observed P-XRD pattern after calcination at 500 °C indicates formation of monoclinic NaV_6O_{15} with NaV_3O_8 as an impurity phase. The phases, NaV_6O_{15} and NaV_3O_8, in the P-XRD pattern are marked by # and *****, respectively.

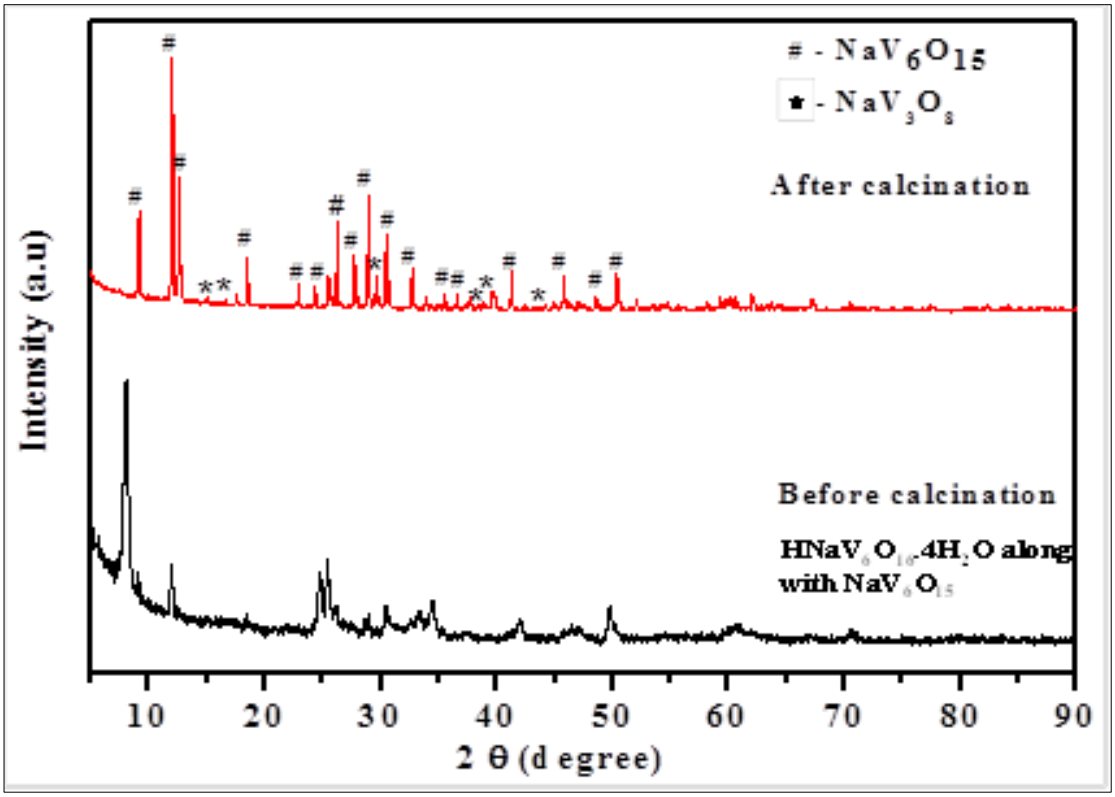

Fig 1: P-XRD patterns of product obtained after calcination (NaV_6O_{15}admixed with NaV_3O_8) and product obtained before calcination ($HNaV_6O_{16}.4H_2O$ along with NaV_6O_{15}).

3.1.2 P-XRD pattern of NaV_6O_{15}

The P-XRD patterns obtained for the Na_2 V_3O_7 stoichiometric preparation using hydrazine hydrate as a reducing agent is shown in Figure 3.2. The analysis of observed P-XRD indicates the formation of pure phase monoclinic NaV_6O_{15} matching with JCPDS PDF No. 24-1155. Figure 3.2 shows the P-XRD patterns recorded before and after the calcination. All the peaks are indexable in the space group *A*2/*m* with the refined lattice parameters, a = 10.151(5) Å, b = 3.606(2) Å, c = 15.581(1) Å and β = 109.45°.

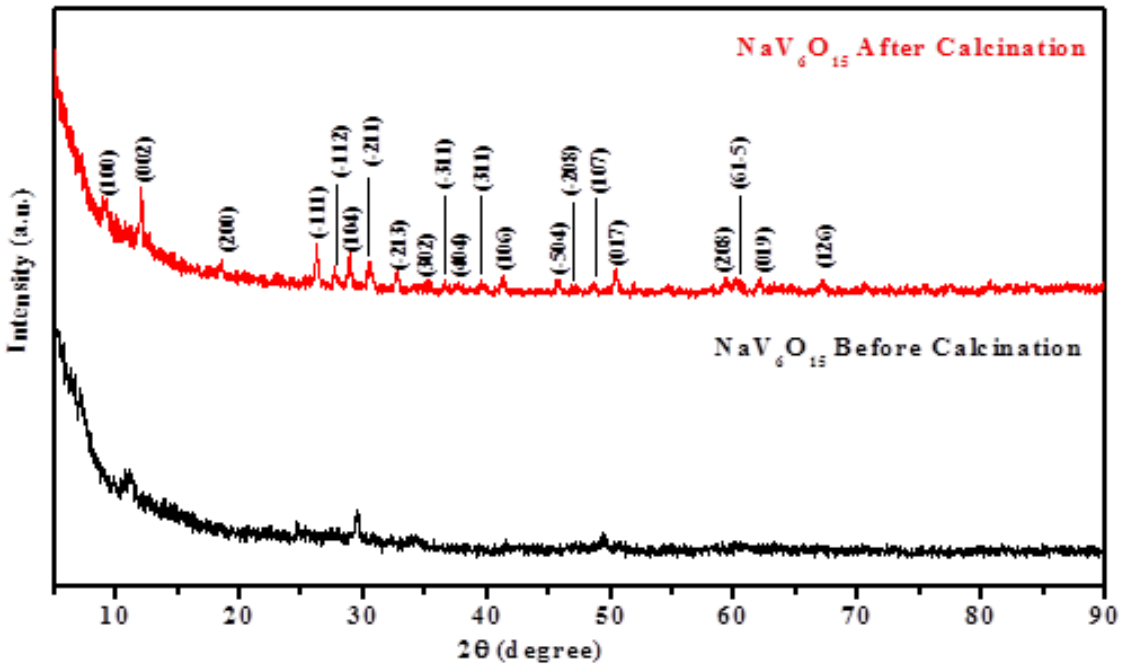

Figure 2. P-XRD patterns of NaV_6O_{15} before and after calcination

3.1.3 P-XRD pattern of $Li_{0.6}V_{1.6}O_{3.67}.H_2O$

The obtained P-XRD pattern indicates that all the diffraction peaks are well matched with $Li_{0.6}V_{1.6}O_{3.67}.H_2O$ phase with the JCPDS PDF No. 48-1152 (*I*4/*mmm* space group – tetragonal). Refined lattice parameters of $Li_{0.6}V_{1.6}O_{3.67}.H_2O$ are, a = 3.712(1) and c = 15.96(1) Å.

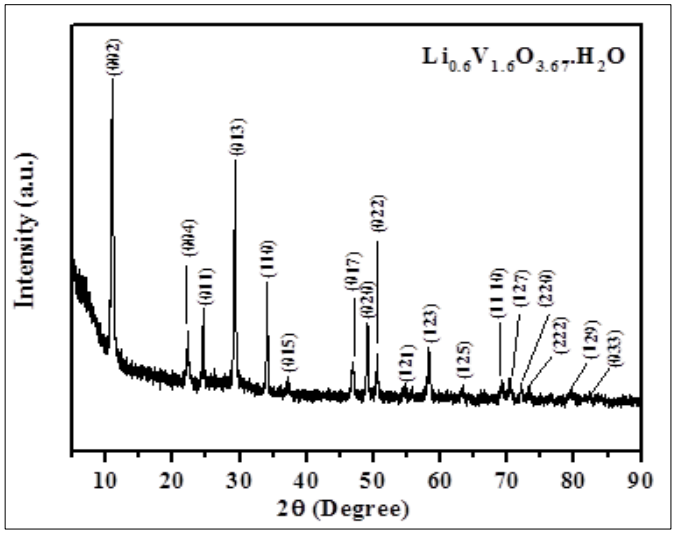

Fig 3: P-XRD pattern of $Li_{0.6}V_{1.6}O_{3.67}.H_2O$ phase.

3.2 FE-SEM Analysis

Powder samples formed by using oxalic acid as reducing agent shows morphology of rectangular shaped rods with two phases, namely, NaV_6O_{15} and NaV_3O_8, while the pure phase of NaV_6O_{15} formed with hydrazine hydrate as reducing agent also shows rectangular rods with complete homogeneity. The length of rod shaped particles ranges from 5 to 10 µm while the diameter ranges from 0.5 to 1 µm. FE-SEM images of phase pure NaV_6O_{15} and NaV_3O_8 admixed NaV_6O_{15} are shown in Figures 3.4 and 3.5, respectively.

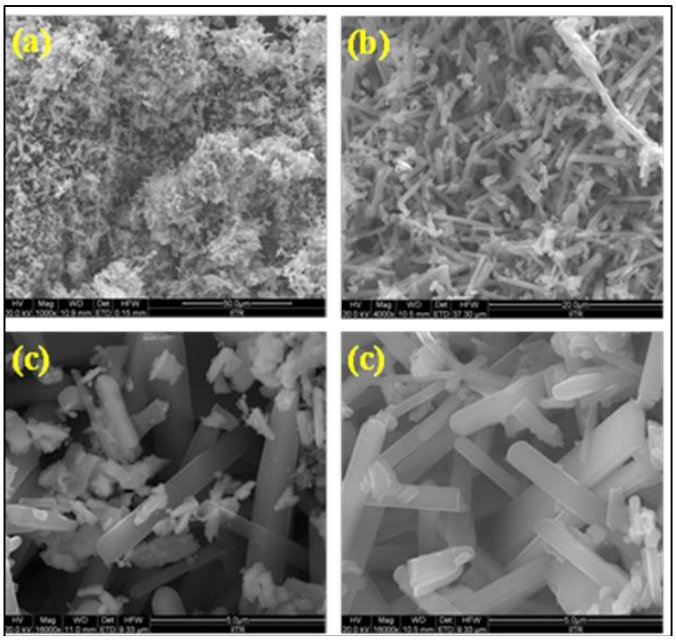

Fig 4: FE-SEM images of NaV_6O_{15} pure phase at magnifications (a) 1000X, (b) 4000X, (c) 16000X

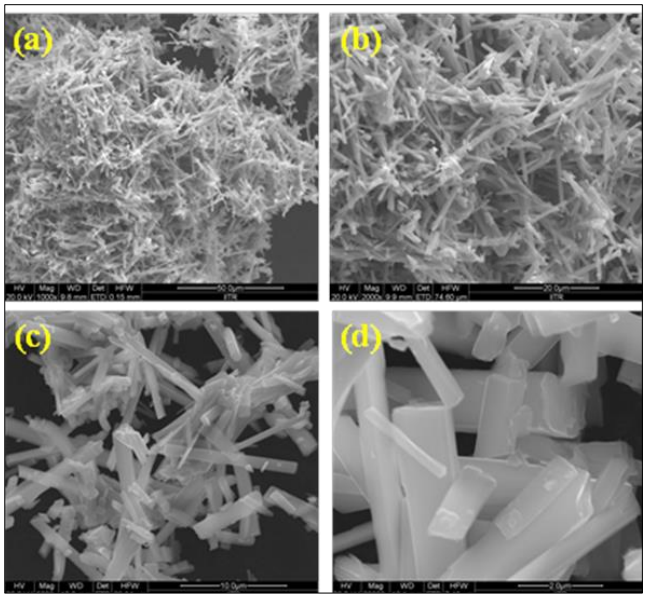

Fig 5: FE-SEM images of NaV_6O_{15} and NaV_3O_8 mixed phase at magnifications (a) 1000X, (b) 2000X, (c) 5000X, (d) 20000X

4. Conclusion

Attempts made to synthesize $Na_2V_3O_7$ and $LiVO_3$ by using a template free modified solvothermal method with ethylene glycol-water solvent system (EG: H_2O; 2:1 *v/v*). The as obtained compounds after the solvothermal reactions were calcined to remove any retained organic substance or solvent molecules and improve crystallinity of the final products. The solvothermal reaction with $Na_2V_3O_7$ stoichiometry resulted in the formation of NaV_6O_{15} admixed with NaV_3O_8 when oxalic acid was used as the reducing agent, while phase pure $NaV_6O_{15}$was obtained when hydrazine hydrate was used as the reducing agent. Therefore, it was believed that hydrazine hydrate works as a better reducing agent in the present solvent and metal system and produces phase pure $NaV_6O_{15}$with reduced vanadium. Both, the phase pure and NaV_3O_8 admixed NaV_6O_{15} forms with rod shaped morphology with an average length of 7 µm and diameter of 0.5 µm. Our attempt to synthesize $LiVO_3$ resulted in the formation of $Li_{0.6}V_{1.6}O_{3.67}.H_2O$ with a highly crystalline tetragonal structure. It will further be interesting to investigate the microstructure and porosity of these materials for their potential uses in Li-ion batteries. Further work will help in optimizing their morphology and appropriate porosity for improved electrochemical properties.

5. Acknowledgements

Jaideep Malik and Jogender gratefully acknowledge the financial assistance provided by UGC, New Delhi in the form of Senior Research Fellowships

6. Conflict of interest: The authors have no conflict of interest.

7. References

1. Armand M, Tarascon JM. Building better batteries. Nature 2008;451:652-657.
2. Palacin MR. Recent advances in rechargeable battery materials: a chemist's perspective. Chem. Soc. Rev 2009;38:2565-2575.
3. Nitta N, Wu F, Lee JT, Yushin G. Li-ion battery materials: present and future. Mater. Today 2015;18:252-264.
4. Goodenough JB, Kim Y. Challenges for rechargeable Li batteries. Chem. Mater 2010;22:587-603.
5. Hwang JY, Myung ST, Sun YK. Sodium-ion batteries: present and future. Chem. Soc. Rev 2017;46:3529-3614.
6. Ohzuku T, Ueda A. Why transition metal (di) oxides are the most attractive materials for batteries. Solid State Ionics 1994;69:201-211.
7. Guo Q, Ma Y, Chen T, Xia Q, Yang M, Xia H, *et al.* Cobalt sulfide quantum dot embedded N/S-doped carbon nanosheets with superior reversibility and rate capability for sodium-ion batteries. ACS nano 2017;11:12658-12667.
8. Wang Q, Xu J, Zhang W, Mao M, Wei Z, Wang L, *et al.* Research progress on vanadium-based cathode materials for sodium ion batteries. J. Mater. Chem. A 2018;6:8815-8838.
9. Jiang H, Hu Y, Guo S, Yan C, Lee PS, Li C. Rational design of MnO/carbon nanopeapods with internal void space for high-rate and long-life Li-ion batteries. ACS nano 2014;8:6038-6046
10. Dai J, Zhu X, Liu J, Wang Q, Li W, Qi Y Russ. J Phys. Chem 2019;93:10.
11. Su D, Wang G, ACS Nano 2013;7:11218.
12. Su WD, Dou SX, Wang GX. J Mater. Chem. A 2014;29:11185.
13. Liang S, Zhou J, Fang G, Zhang C, Wu J, Tang Y *et al*, Electrochem. Acta 2014;130:119.
14. He H, Zeng X, Wang H, Chen N, Sun D, Tang Y, Pan Y. J Electrochem. Soc 2015;162:A39.
15. Yuan S, Zhao Y, Wang Q. J Alloys Compd 2016;688:55.
16. Yuan S, Liu YB, Xu D, Ma DL, Wang S, Yang XH *et al*. Zhang, Adv. Sci 2015;2:1400018.
17. Ni S, Lv X, Ma J, Yang X, Zhang L. J Power Sources 2014;248:122.
18. Das SK, Darmakolla S, Bhattacharyya AK. J Mater. Chem 2010;20:1600.
19. Wang D, Choi D, Yang Z, Viswanathan VV, Nie Z, Wang C, *et al.* Chem. Mater 2008;20:3435.
20. Kim TW, Kleitz F, Paul B, Ryoo R. J Am. Chem. Soc 2005;127:7601.
21. Zhao D, Feng J, Huo Q, Melosh N, Fredrickson GH, Chmelka BF, Stucky GD. Science, 1998;279:548.
22. Ke FS, Huang L, Wei HB, Cai JS, Fan XY, Yang FZ *et al*. Power Sources 2007;170:450.
23. Kim JM, Huh YS, Han YK, Cho MS, Kim H. J Electrochem. Comm 2012;14:1932.
24. Lee KH, Song SW. Appl. Mater. Interfaces 2011;3:3697.
25. Qu B, Zhang M, Lei D, Zeng Y, Chen Y, Chen L, *et al.* Nanoscale 2011;3:3646.
26. Wang S, Lu Z, Wang Da, Li C, Chen C, Yin Y, Mater J. Chem 2011;21:6365